

Second-order elastic constants for the Lennard-Jones solid

Michiel Sprik, Roger W. Impey, and Michael L. Klein

Chemistry Division, National Research Council of Canada, Ottawa, Canada K1A 0R6

(Received 29 November 1983)

The elastic constants of a classical nearest-neighbor Lennard-Jones solid are evaluated with the use of molecular-dynamics calculations in order to make comparisons with similar quantities derived from Monte Carlo calculations. Following Parrinello and Rahman, we use both strain fluctuations in the (p, H, N) ensemble and uniaxial loading to obtain the adiabatic elastic compliances and hence the elastic constants. While there is broad agreement between the three methods, Monte Carlo evaluation seems to be the most efficient procedure. The relationship between the elastic constants of the fcc and hcp solids is also discussed.

I. INTRODUCTION

Elastic constants are important not only because they provide a link between the mechanical and dynamic behavior of crystals but also because they are a means of probing the interatomic forces.¹ This latter property has been widely exploited, particularly in the case of the solid rare gases.² There, for example, the intercomparison of Monte Carlo calculations based upon realistic two-body potentials³ with experimental data² has revealed the importance of three-body forces. For such comparison to be meaningful it is necessary not only to have accurate experiment data,² but also to have a reliable method of calculating the elastic constants for a given interatomic potential. At high temperatures, where anharmonic effects are important and quantum effects are small, classical Monte Carlo calculations are generally considered to be the best way to evaluate the elastic constants.^{3,4} Recent advances in computer-simulation techniques have indicated how, in principle, molecular-dynamics calculations can also be used to obtain the elastic constants.⁵⁻⁷ The new method depends upon the evaluation of strain fluctuations in the (p, H, N) ensemble, which determine the adiabatic compliances, and these in turn yield the elastic constants.⁶ Moreover, the new method appears to be equally applicable to both ordered (crystalline) and disordered (amorphous) materials.⁶ However, to date, no intercomparison has been made of the relative merits of the canonical ensemble Monte Carlo method⁸ and the (p, H, N) ensemble molecular dynamics (NMD) approach.⁶ Such intercomparisons are best initially carried out for simple (idealized) model systems, and this is the purpose of the present paper. In particular, we present NMD results on the elastic constants of both the face-centered cubic⁹ (fcc) and hexagonally close-packed (hcp) solids¹⁰ whose constituent atoms interact with a nearest-neighbor Lennard-Jones interatomic potential.⁹ In effect, we are dealing with an idealized model of the rare-gas solids.¹¹ The relevant theory is presented in the next section and the results of our NMD calculations are given in Sec. III. In addition to exploiting the strain fluctuations,⁶ we also present results based upon uniaxial loading of the sample.⁵⁻⁷ While these two methods agree with each other, comparison with Monte

Carlo results for the same model indicates that the NMD method appears to require larger amounts of computer time in order to obtain reliable values of the elastic constants. The paper ends with a discussion.

II. OUTLINE OF THEORY

In order to simulate the behavior of a system of particles under conditions of constant external stress, the time dependence of three basic vectors $\vec{a}(t)$, $\vec{b}(t)$, $\vec{c}(t)$ specifying the edges of the MD cell are followed.^{5,6} For convenience, these vectors are arranged in a 3×3 matrix \underline{h} . The time evolution of the $3N$ particle coordinates $\{\vec{r}(t)\}$ and the matrix \underline{h} is obtained from the Parrinello-Rahman Lagrangian^{5,6}

$$L = \frac{1}{2} \sum_i m_i \dot{\vec{s}}_i' \underline{G} \dot{\vec{s}}_i - V + \frac{1}{2} \mathcal{W} \text{Tr}(\dot{\underline{h}}' \dot{\underline{h}}) + V_{\text{el}}, \quad (1)$$

where $\vec{r} = \underline{h} \vec{s}$, $\underline{G} = \underline{h}' \underline{h}$, and a prime indicates a transpose. \mathcal{W} is the mass associated with the coordinates $h_{\lambda\mu}$. V is the potential energy determining the interaction between the particles. Periodic boundary conditions are applied with respect to the moving MD cell boundaries defined by \underline{h} . V_{el} denotes the elastic energy of the system, which depends on the applied stress \underline{S} and the strain $\underline{\epsilon}$. In the present study we consider only systems under zero hydrostatic pressure. Under these conditions V_{el} is written as

$$V_{\text{el}} = \Omega_0 \text{Tr}(\underline{S} \underline{\epsilon}), \quad (2)$$

where $\Omega_0 = |\underline{h}_0|$ is the unstrained volume. The derivation of a closed set of dynamical equations for the $3N + 9$ coordinates $\{\vec{r}, \underline{h}\}$ from the Lagrangian (1) requires the strain tensor $\underline{\epsilon}$ to be expressed in terms of these coordinates. Noting the intimate connection between the metric tensor \underline{G} and the notion of strain, Parrinello and Rahman^{5,6} identified the strain as

$$\underline{\epsilon}(t) = \frac{1}{2} [\underline{h}'_0^{-1} \underline{G}(t) \underline{h}_0^{-1} - \underline{1}]. \quad (3)$$

Here $\underline{G}(t)$ is the instantaneous value of the metric tensor in the strained state, and \underline{h}_0 is the average of the matrix determining the MD cell in the reference state. The strain tensor (3) describes therefore a homogeneous deformation

fluctuating in time. It can be shown that the dynamics generated by the Lagrangian (1) with (2) conserves the enthalpy H . Time averages over a sufficiently long MD trajectory therefore correspond to expectation values with respect to the constant (S, H, N) ensemble. The equilibrium fluctuations of strain in this ensemble are related to the adiabatic compliances Γ_{ijkl}^s according to^{5,6}

$$\langle \Delta \epsilon_{ij} \Delta \epsilon_{kl} \rangle_{S, H, N} = \frac{k_B T}{\Omega_0} \Gamma_{ijkl}^s. \quad (4)$$

The relations (4) enable us to determine the elastic compliances from the time-averaged fluctuations of the strain (3) in the reference state. A second and independent method for the evaluation of the Γ_{ijkl}^s is to apply stress to the sample and measure the resulting average strain. Provided the deformation, starting from the reference state, is performed quasistatically and reversibly, the Γ_{ijkl}^s follow immediately from the linear elastic relations

$$\langle \epsilon_{ij} \rangle = \sum_{k,l} \Gamma_{ijkl}^s S_{kl}. \quad (5)$$

Clearly the values obtained through the relations (4) and (5) should be identical and a comparison of the two sets of estimates from a MD calculation is a powerful tool to investigate the accuracy of the constant stress simulation method. A further test for this approach is a comparison with the results of constant temperature, constant volume (strain) Monte Carlo calculations. The strain in the (V, T, N) ensemble is defined in terms of the fixed lattice basis vectors.⁸ Since the lattice basis vectors and the MD cell vectors are proportional for a given system, the strain as defined in Ref. 8 can be equally written in terms of the matrix \underline{h} . The result is an expression identical to Eq. (3), except that the metric matrix \underline{G} is time independent in the (ϵ, T, N) ensemble and imposed on the system by the constraints of the MD cell in the deformed state. The strain in the (ϵ, T, N) ensemble should therefore be compared to the expectation value of the strain in the corresponding (S, H, N) ensemble. However, because of the correlations in the motion of the matrix \underline{h} we have

$$\begin{aligned} \langle \underline{\epsilon} \rangle &= \frac{1}{2} (\underline{h}'_0)^{-1} \langle \underline{h}' \rangle \langle \underline{h} \rangle \underline{h}_0^{-1} - \underline{\mathbb{1}} \\ &+ \frac{1}{2} (\underline{h}'_0)^{-1} \langle \Delta \underline{h}' \Delta \underline{h} \rangle \underline{h}_0^{-1}. \end{aligned} \quad (6)$$

The first term in (6) corresponds to the strain in the (ϵ, T, N) ensemble (apart from possible ensemble corrections for the expectation value of \underline{h}). The second term is in general finite in a small sample. As a consequence of this correction term the expectation value of the strain remains finite in the reference state. However, the correction term vanishes in the thermodynamic limit as may be justified by the following scaling argument. The matrix \underline{h} behaves like the dimension of the system in one direction. Hence we may write

$$\langle \underline{h} \rangle = O(N^{1/3}), \quad \langle \Delta \underline{h}' \Delta \underline{h} \rangle = O(N^{1/3}), \quad (7)$$

from which it follows that

$$\underline{h}'_0^{-1} \langle \Delta \underline{h}' \Delta \underline{h} \rangle \underline{h}_0^{-1} = O(N^{-1/3}). \quad (8)$$

The relation (8) implies that the convergence of the MD

result with increasing system size is rather slow. The system size dependence will affect the estimates for the compliances through the fluctuation relation even more seriously because the left-hand side of Eq. (4) involves a fourth moment of \underline{h} . For the purpose of a consistent comparison of the compliances obtained from fluctuations and the linear elastic relations (5), we have therefore included the correction term for the reference state in the definition of strain. We therefore write

$$\underline{\epsilon} = \frac{1}{2} \underline{h}'_0^{-1} (\underline{G} - \underline{G}_0) \underline{h}_0^{-1}, \quad (9)$$

where \underline{G}_0 denotes the expectation value of the metric tensor in the reference state. The modified form (9) has the advantage that the average strain vanishes in the reference state of a finite sample.

The two methods discussed in this section both give the compliances Γ_{ijkl}^s rather than the elastic constants C_{ijkl}^s . On the other hand, the (ϵ, T, N) Monte Carlo approach yields directly estimates of the elastic constants.^{8,10} We will, therefore, end this section with a brief comment on the way the C_{ijkl}^s are derived from the Γ_{ijkl}^s . Because of the permutation symmetry for the Cartesian indices the 9×9 matrix Γ_{ijkl}^s is singular. Hence, in order to invert the linear relations (5) the matrix Γ_{ijkl}^s must be reduced to a nonsingular 6×6 matrix $\Gamma_{\rho\sigma}^s$. Using the familiar Voigt convention¹ to relate the indices ρ and i, j we have

$$\Gamma_{\rho\sigma}^s = \begin{cases} \Gamma_{ijkl}^s, & k=l \ (\sigma \leq 3) \\ 2\Gamma_{ijkl}^s, & k \neq l \ (\sigma > 3) \end{cases}. \quad (10)$$

Note that the matrix $\Gamma_{\rho\sigma}^s$ is no longer symmetric. The inverse of $\Gamma_{\rho\sigma}^s$ again is a nonsymmetric 6×6 matrix. The symmetric 9×9 matrix of elastic constants C_{ijkl}^s in the Cartesian representation is then obtained from the inverse of $\Gamma_{\rho\sigma}^s$ by the inverse transformation (1). As an application we note that the shear elastic constant C_{44}^s in a cubic system is found to be one-fourth the reciprocal of the corresponding compliance.

III. RESULTS FOR THE ELASTIC CONSTANTS

A. Strain fluctuations

As an application of the methods outlined in the preceding section, we present the result of constant pressure MD simulations on a system of argon atoms interacting with a Lennard-Jones nearest-neighbor interaction ($\epsilon_0 = 119.8$ K, $\sigma = 3.805$ Å). The basic simulations were performed for a face-centered cubic (fcc) system of $N = 256$ particles at reduced temperatures ($k_B T / \epsilon_0$) of approximately 0.3 and 0.5. By using these data for a comparison, several of the relevant parameters (viz. the system size, the value of W [see Eq. (1)], and temperature) were varied. The results for three independent runs for the $N = 256$ system are presented in columns *A*, *B*, and *C* of Table I. All the calculations employed a third-order Gear algorithm along with a time step of 8.6 fs. The mass W associated with the \underline{h} matrix was set equal to the mass of a single argon atom. This value of W yields an optimal coupling between the motion of the boundaries of the MD cell and the particles of the system. Figure 1 shows the

TABLE I. Comparison of low-temperature elastic constants (in units of $Nk_B T/V$) derived from strain fluctuations with Monte Carlo results for a fcc lattice with nearest-neighbor Lennard-Jones (12-6) interactions. The number in parentheses gives the number of MC steps per particle.

MD run	A	B	C	D	E	Cowley ^a
System size, N	256	256	256	108	108	108
No. of steps/ 10^3	50	50	40	100	50	(25)
$k_B T/\epsilon_0$	0.3093	0.3131	0.3101	0.3065	0.3068	0.3100
R/σ	1.1497	1.1502	1.1498	1.1498	1.1499	1.1495
$\langle \Phi \rangle / Nk_B T$	-17.649	-17.413	-17.605	-17.817	-17.802	
C_p / Nk_B	3.52	3.52	3.38	3.65	3.45	3.54 ± 0.04
B_s	124	112	123	112	121	119.1 ± 0.5
$\frac{1}{3}(C_{11} + C_{22} + C_{33})$	179 ± 8	169 ± 5	180 ± 7	170 ± 9	176 ± 6	175.6 ± 0.5
$\frac{1}{3}(C_{12} + C_{13} + C_{23})$	94 ± 7	84 ± 5	96 ± 3	84 ± 8	93 ± 8	90.8 ± 0.5
$\frac{1}{3}(C_{44} + C_{55} + C_{66})$	79.3 ± 1.5	73 ± 11	83 ± 13	81.7 ± 1.3	79 ± 8	79.0 ± 0.2
$Nk_B T/V$ (kbar)	0.120 59	0.121 91	0.120 86	0.119 49	0.119 59	

^aReference 9.

averages of the elastic constants for the run labeled *A* in Table I as a function of the number of time steps over which they were evaluated. The results were obtained by inverting the compliance matrix as determined from the strain fluctuations according to Eq. (4). The individual C_{ij}^s which are required to be identical by cubic symmetry are also plotted. The data in Table I represent averages over the three symmetry-related C_{ij}^s evaluated at the end of the run. It is clear from Fig. 1 that the convergence with an increasing number of time steps is disappointingly

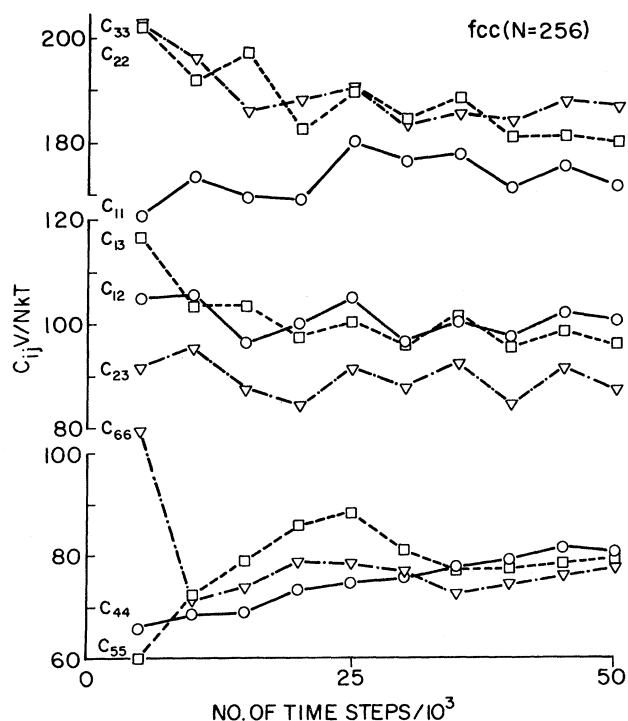


FIG. 1. Adiabatic elastic constants (in reduced units) for an fcc system of $N = 256$ Ar atoms as a function of the number of time steps for $W = m_{Ar}$. The data are for run *A* of Table I.

slow. The MD run had to be continued well beyond 10^4 time steps in order to obtain an accuracy better than 10%. A similar convergence was found for the specific heat. In addition, there seems to be a persistent discrepancy between the values of the symmetry-related C_{ij}^s even after 5×10^4 time steps which may be due to a small but stable residual distortion of the cell from cubic symmetry. This perturbation, negligible for structural properties such as lattice constants, is magnified to a considerable degree for the C_{ij}^s . The disagreement between the three symmetry-related C_{ij}^s can be used to estimate the statistical errors, and the errors quoted in Table I are the standard deviations with respect to the average over symmetry-equivalent quantities. A comparison with the results of the two independent runs *B* and *C* gives a further estimate of the errors. From this we conclude that the precision obtained for a simulation with this particular set of parameters is of the order of 5%. The columns *D* and *E* contain data for a fcc sample of 108 particles. Figure 2 shows accumulative averages of C_{11}^s , C_{22}^s , and C_{33}^s for run

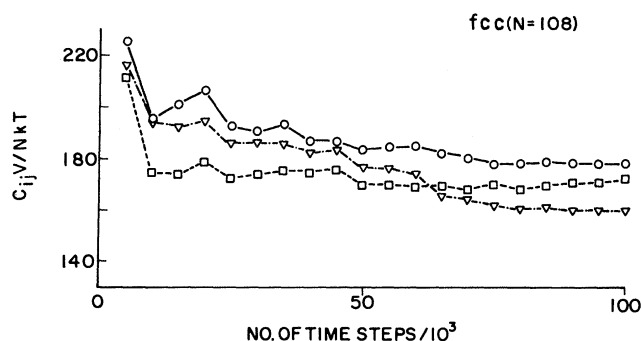


FIG. 2. Adiabatic elastic constants C_{11}^s (circles), C_{22}^s (squares), C_{33}^s (triangles) for an fcc system of $N = 108$ Ar atoms as a function of the number of time steps over which the averages are evaluated for $W = m_{Ar}$. The data are for run *D* of Table I.

TABLE II. Comparison of high-temperature elastic constants in units of $Nk_B T/V$ derived from strain fluctuations with Monte Carlo results for an fcc lattice with nearest-neighbor Lennard-Jones (12-6) interactions. The number in parentheses gives the number of MC steps per particle.

MD run	A	B	Cowley ^a
System size, N	256	256	108
No. of steps/ 10^3	50	50	(25)
$k_B T/\epsilon_0$	0.5089	0.5076	0.5090
R/σ	1.1773	1.1770	1.1759
$\langle \Phi \rangle / Nk_B T$	-9.779	-9.814	-9.794
C_p / Nk_B	4.13	4.36	4.33
B_s	57	57	55.5 ± 0.4
$\frac{1}{3}(C_{11} + C_{22} + C_{33})$	80 ± 3	81.7 ± 1	80.5 ± 0.4
$\frac{1}{3}(C_{12} + C_{13} + C_{23})$	45 ± 2	44.3 ± 1	42.9 ± 0.4
$\frac{1}{3}(C_{44} + C_{55} + C_{66})$	32 ± 2	32.0 ± 1	32.3 ± 0.2
$Nk_B T/V$ (kbar)	0.184 83	0.184 48	

^aReference 9.

D. The convergence for the smaller sample is worse but a possible number dependence of the final averages seems to be well below the errors introduced from other sources, and no quantitative estimate of the N dependence could be determined. Increasing the mass W by a factor of 10 has serious consequences for the convergence as can be seen from Fig. 3 for $N=256$. The response of the MD cell boundaries to the motion of the particles has become considerably slower, and no reliable values for the C_{ij}^s can be derived in a run of 50×10^3 steps. Another variable that may be relevant to the accuracy is temperature. Results for the $N=256$ system at the reduced temperature of 0.5 are presented in Fig. 4 and Table II. The convergence of the averages with the number of time steps is no different from the lower-temperature data shown in Fig. 1. However, the (relative) systematic error due to the persistent non-cubic perturbation seems to be slightly less (see also Table II).

B. Stress-strain relations

To investigate the validity of the linear relations (5), a stress was applied to several of the runs quoted in Tables I and II, by using the last time step of each as a starting point and reference state. Some of the results are shown in Figs. 5 and 6. The stress was increased in stages, each having a typical run length of $5 \times 10^3 - 10 \times 10^3$ time steps; the stress was then decreased again in stages. No irreversible hysteresis effects were observed, and within the errors mentioned before the samples recovered cubic symmetry. The straight lines in Figs. 5 and 6 are the linear relations as predicted by the compliances obtained from the equilibrium fluctuations in the reference state. For a more quantitative comparison the points in the stress-strain cycle have been fitted to a straight line. Because the strain in the reference state (zero stress) vanishes by definition [see Eq. (9)], the line is forced to go through the origin. When a set of strain components could be as-

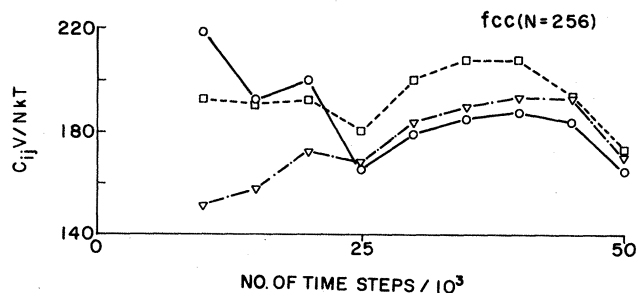


FIG. 3. Adiabatic elastic constants C_{11}^s (circles), C_{22}^s (squares), C_{33}^s (triangles) for an fcc system of $N=256$ atoms as a function of the number of time steps over which the averages are evaluated for $W=10m_{Ar}$.

sumed to be identical by symmetry, the "experimental" values were averaged and taken as one point in the linear regression. The error estimates of the least-mean-square procedure were used as a measure for the statistical errors of the C_{ij}^s derived from the stress cycles. Table III gives the results along with values of the C_{ij}^s in the reference state from Tables I and II. The agreement is within the statistical error. However, the errors for C_{11}^s and C_{12}^s as obtained from the linear elastic relations are considerable. As with the results in Tables I and II, the C_{ij}^s from the stress-strain relations show no significant N dependence.

For a comparison of the efficiency of the two methods we note that the total length in time steps of the stress cy-

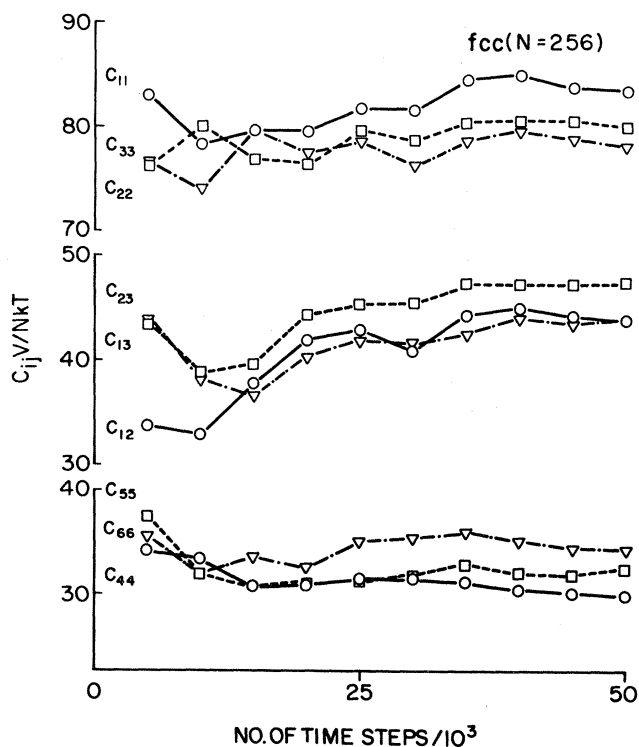


FIG. 4. Adiabatic elastic constants (in reduced units) for an fcc system of $N=256$ Ar atoms as a function of the number of time steps for $W=m_{Ar}$. The data are for run A of Table II.

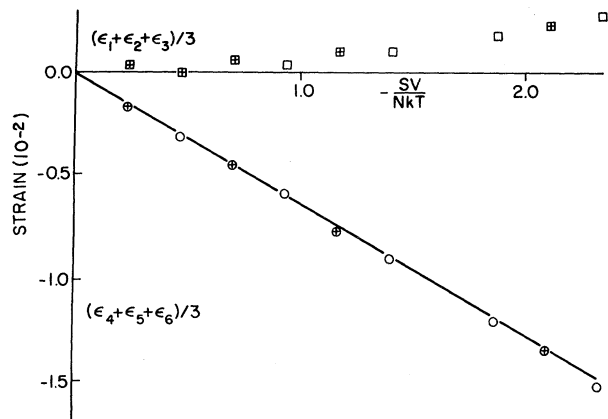


FIG. 5. Effect of shear stress applied to an fcc solid (run *A* of Table I). S gives the value of the nonzero stress components $S_4=S_5=S_6$. The open symbols are strains obtained with increasing stress; the symbols with a cross were obtained with decreasing stress. The straight line gives the linear elastic relations as predicted from the equilibrium fluctuations in the reference state. Note that the nonvanishing value of the ϵ_1 , ϵ_2 , and ϵ_3 is a nonlinear effect.

cles is about equal to the length of the runs in the reference state. However, applying stress breaks the cubic symmetry. This implies that the accuracy for C_{11}^s can no longer be improved by averaging over symmetry. This effect is one of the origins of the larger errors in C_{11}^s and C_{12}^s obtained from uniaxial loading. Moreover, two different stress cycles are needed for a determination of a full set of Γ_{ijkl}^s , i.e., uniaxial loading as well as shearing. For a crystal with lower symmetry than cubic (see below) the system must be subjected to stress in additional independent directions. Hence we may conclude from these considerations that an evaluation of the C_{ij}^s from equilibrium fluctuations is the more efficient method.

For a comparison of the NMD approach to the (N, V, T) Monte Carlo (MC) method⁴ the last column of Tables I and II contains the results of Cowley,⁹ for a nearest-neighbor Lennard-Jones model of solid argon. (A small temperature correction has been applied to the data of Ref. 9.) The MC averages were obtained for a system of 108 particles with about 20×10^3 configurations per particle. This makes the length of the MC calculation comparable to the length of the MD runs in Tables I and II. The agreement is satisfying particularly for the high-

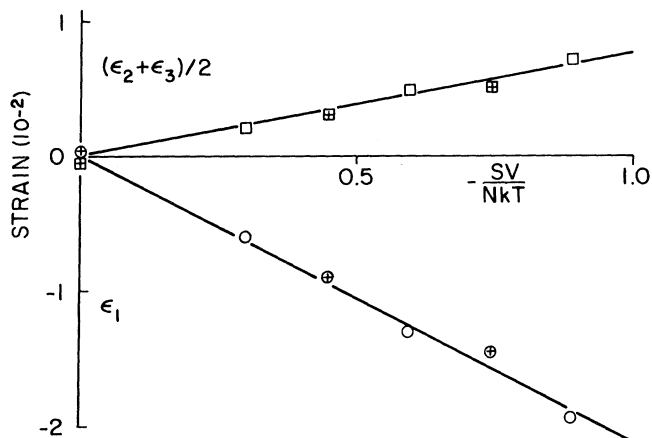


FIG. 6. Effect of stress loading along the X axis of an fcc solid (run *A* of Table II). The symbols have the same meaning as in Fig. 5.

temperature C_{ij}^s . However, the precision claimed for the MC calculation is an order of magnitude better than our MD results. This clearly implies that the MC method is the more efficient procedure. We will return to this point in the Discussion section.

C. hcp argon

A system of argon atoms, with the same nearest-neighbor interaction as before, was set up in a hexagonal close-packed (hcp) lattice. As is well known from literature,¹⁰ the hcp elastic constants and the fcc constants measured with respect to an equivalent reference frame are almost indistinguishable. This enables us to examine the hcp elastic constants by comparing them to the equivalent fcc values. The first column of Table IV lists the C_{ij}^s obtained from the equilibrium fluctuations in a hcp sample of $N=250$ particles. Figure 7 shows the averages of the C_{ij}^s as a function of the number of time steps. Despite the effect of the perturbation from perfect symmetry discussed before, the reduction of cubic to hexagonal symmetry is evident from the splitting in the manifold of three C_{ij}^s identical in a cubic system. In particular, for C_{33}^s , the coefficient for loading along the c axis, the convergence is rather poor. The second column in Table IV gives the results for a $N=150$ particle system. The size of this system in the c direction is $\frac{3}{5}$ the size of the larger one. The

TABLE III. Comparison of elastic constants for fcc argon (in units of $Nk_B T/V$) derived from fluctuations and stress-strain relations.

Elastic constants	$N=256$ ($Nk_B T/V=0.1848$ kbar)		$N=256$ ($Nk_B T/V=0.1206$ kbar)		$N=108$ ($Nk_B T=0.1195$ kbar)	
	Fluctuations	Stress-strain	Fluctuations	Stress-strain	Fluctuations	Stress-strain
$\frac{1}{3}(C_{11}+C_{22}+C_{33})$	80 ± 3	84 ± 12	179 ± 8	197 ± 24	170 ± 9	188 ± 17
$\frac{1}{3}(C_{12}+C_{13}+C_{23})$	45 ± 2	48 ± 12	94 ± 7	111 ± 24	84 ± 8	99 ± 16
$\frac{1}{3}(C_{44}+C_{55}+C_{66})$	32 ± 2	32.5 ± 1.5	79.3 ± 1.5	77.2 ± 0.3	81.7 ± 0.3	77.1 ± 0.9

TABLE IV. A comparison between hcp and transformed frame fcc elastic constants in units of $Nk_B T/V$ derived from strain fluctuations.

MD run	A	B	A (fcc)
System size, N	250	150	256
No. of steps/ 10^3	50	50	50
$k_B T/\epsilon_0$	0.3091	0.3054	0.3093
R/σ	1.1496	1.1493	1.1497
c/a	1.6337	1.6338	
$\langle \Phi \rangle / Nk_B T$	-17.675	-17.901	-17.649
C_p / Nk_B	3.54	3.59	3.52
B_s	128	115	124
$\frac{1}{2}(C_{11} + C_{22})$	217 ± 5	202 ± 4	215 ± 10
C_{33}	250	241	228 ± 11
C_{12}	88.5	76	82 ± 4
$\frac{1}{2}(C_{13} + C_{23})$	72 ± 3	58 ± 4	70 ± 3
$\frac{1}{2}(C_{44} + C_{55})$	53 ± 2	57 ± 0.5	55 ± 2
C_{66}	68	62	67 ± 3
$Nk_B T/V$ (kbar)	0.120 52	0.119 16	0.120 59

C_{ij}^s for the smaller sample seem to be slightly lower. However, this difference may not be significant because the errors ($\sim 10\%$) for the hcp C_{ij}^s are considerably larger than for the fcc system. This is confirmed by a comparison with values obtained from stress-strain cycles applied to the hcp system (see Table V). Since not all independent Γ_{ij}^s necessary for an inversion have been measured, compliances are compared in Table V rather than elastic constants. The last column of Table IV gives the fcc C_{ij}^s obtained from sample A in Table I, transformed to the proper frame.¹⁰ For technical reasons related to the constant-pressure MD program, this frame was not quite the same as the trigonal frame introduced in Ref. 10. An additional rotation of $\pi/12$ about the c axis is required. However, it turns out that the constants listed in the tables are invariant under this rotation and the transformation rules as given in Ref. 10 are still valid. But the constant coupling uniaxial loading and shearing are different in the two frames. This implies that the corrections for internal strain must be modified. For this reason the transformed fcc constants presented in Table IV have not been correct-

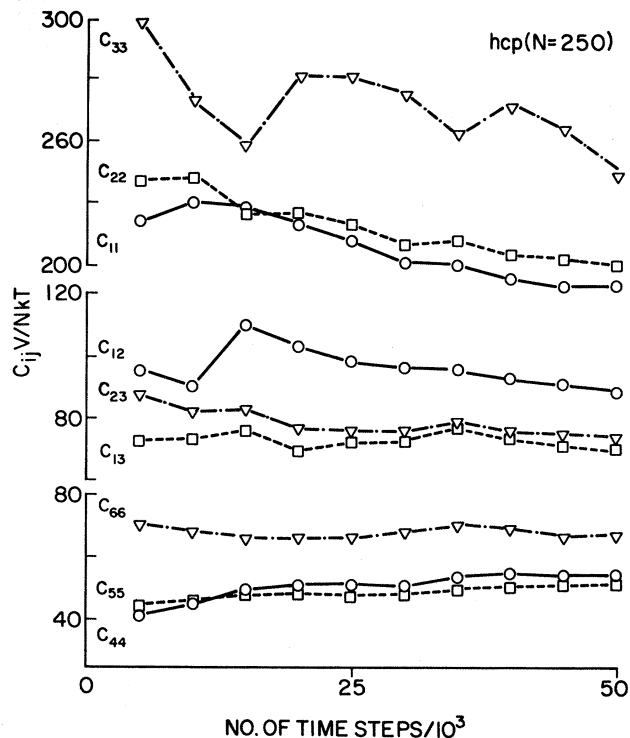


FIG. 7. Adiabatic elastic constants (in reduced units) for an hcp system of $N=250$ Ar atoms as a function of the number of time steps for $W = m_{Ar}$. The data are for run A of Table IV.

ed for internal strain. Within the errors mentioned above there is no distinction between the fcc and hcp system. The internal strain corrections evaluated according to Ref. 10 can be used as an order of magnitude estimate of the strain corrections, despite the fact that they are evaluated in a slightly different frame. We conclude that the internal strain may be neglected in view of larger errors involved in the determination of the C_{ij}^s .

IV. DISCUSSION

We have presented the results of molecular-dynamics calculations of the second-order elastic constants of the Lennard-Jones solid with the use of the NMD method.^{5,6} The results have been compared with Monte Carlo calculations employing the (N, V, T) ensemble.^{4,11} Our main finding is that rather lengthy calculations seem to be re-

TABLE V. Comparison of compliances [in units of $10^{-3}(V/Nk_B T)$] derived from fluctuations and stress-strain relations for hcp argon.

Compliance	$N=250$ ($V/Nk_B T = 8.2974$ kbar $^{-1}$)		$N=150$ ($V/Nk_B T = 8.3921$ kbar $^{-1}$)	
	Fluctuations	Stress-strain	Fluctuations	Stress-strain
C_{33}^{-1}	4.6	4.84	4.6	4.9 ± 0.1
$\frac{1}{3}(C_{33}^{-1} + C_{23}^{-1})$	-1.09 ± 0.06	-1.18 ± 0.03	-1.0 ± 0.2	-1.16 ± 0.06
$\frac{1}{2}(C_{44}^{-1} + C_{55}^{-1})$	18.9 ± 0.8	18.5 ± 0.2		
C_{66}^{-1}	14.8	16.3 ± 0.3	16.1	15.9 ± 0.3

quired to obtain elastic constants to 5% accuracy from MD calculations using either fluctuations or the stress-strain relationships. Accordingly, Monte Carlo methods^{8,9} would seem to be the preferred means of calculation.

This conclusion is disappointing since the computer codes for carrying out NMD calculations for molecular systems have already been developed.^{12,13} A natural application of the methods discussed in this article would be the study of the elastic constants of molecular solids in the vicinity of phase transitions. While such calculations remain to be done, the results presented here suggest that prohibitively long calculations will be required. However, at present Monte Carlo calculations have not yet been

used to study the elastic constants of molecular solids. It remains to be established whether or not the pessimistic conclusions for solid Ar can be carried over to the case of molecular crystals where additional relaxation mechanisms (via translation-rotation coupling) exist. Indeed, the determination of a stress free reference state in the (N, V, T) Monte Carlo method is a nontrivial calculation.

ACKNOWLEDGMENT

One of us (M.S.) gratefully acknowledges support by a Natural Sciences and Engineering Research Council (Canada) fellowship. We thank Roger Cowley for useful discussions and for providing us with details of his unpublished calculations.

-
- ¹M. Born and K. Huang, *Dynamical Theory of Crystal Lattices* (Clarendon, Oxford, 1954).
²B. P. Stoicheff, in *Rare Gas Solids*, edited by M. L. Klein and J. A. Venables (Academic, London, 1977), Vol. II.
³M. L. Klein and R. D. Murphy, *Phys. Rev. B* **6**, 2433 (1972).
⁴M. L. Klein and T. R. Koehler, in *Rare Gas Solids*, edited by M. L. Klein and J. A. Venables (Academic, London, 1976), Vol. I.
⁵M. Parrinello and A. Rahman, *J. Appl. Phys.* **52**, 7182 (1981).
⁶M. Parrinello and A. Rahman, *J. Chem. Phys.* **76**, 2662 (1982).
⁷I. K. Schuller and A. Rahman, *Phys. Rev. Lett.* **50**, 1377 (1983).
⁸D. R. Squire, A. C. Holt, and W. G. Hoover, *Physica* **42**, 388 (1969).
⁹E. R. Cowley, *Phys. Rev. B* **28**, 3160 (1983).
¹⁰S. F. Ahmad, H. Kiefte, M. J. Clouter, and M. D. Whitmore, *Phys. Rev. B* **26**, 4239 (1982).
¹¹M. L. Klein and W. G. Hoover, *Phys. Rev.* **4**, 539 (1971).
¹²S. Nosé and M. L. Klein, *Phys. Rev. Lett.* **50**, 1207 (1983); *J. Chem. Phys.* **78**, 6928 (1983).
¹³R. W. Impey and M. L. Klein, *Chem. Phys. Lett.* **103**, 143 (1983).